JOC*Note*

Kinetic Selectivity in the N-Alkylation of 2-Pyridyl Porphyrins: A Facile Approach to the αα*ββ* Scaffold

Ankona Datta, Suzanne M. Quintavalla, and John T. Groves*

Department of Chemistry, Princeton University, Princeton, New Jersey 08544

jtgroves@princeton.edu

Received September 29, 2006

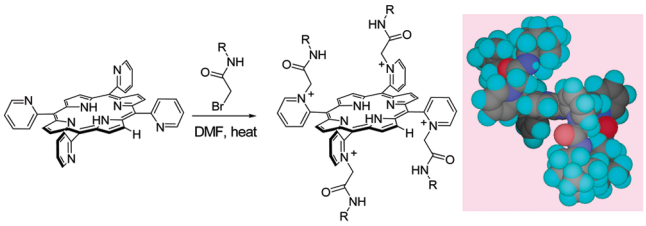

79% αα*ββ* atropisomer (R = (*R*)-bornyl)

meso-Tetrakis(2-pyridyl)-porphyrin (2-PyP) was tetra-*N*-alkylated with three different α-bromoacetamides to generate a series of water-soluble *N*-alkylpyridinium porphyrins (**1**−**3**). The product mixtures showed a marked preference for the formation of the αα*ββ* atropisomer. With α-bromo-*N*-*n*-butylacetamide, the corresponding αα*ββ* 2-tetrakis (*N*-*n*-butylacetamido)-pyridyl porphyrin (2-TnBuPyP, **3**) was obtained in 69% isolated yield in a single step. Prolonged heating lead to equilibration of the rotational isomers for the less bulky alkyl groups, indicating that the observed preference is a kinetic effect. The intermediate products for the *N*-bornyl case were identified by LC/ESI-MS to deduce an explanation for the observed nonstatistical selectivity.

Cationic metalloporphyrins have a wide range of applications as water-soluble oxidation catalysts[1,2] and as hosts for the molecular recognition of small molecules in water.[3,4] Further, some porphyrins of this type have shown considerable promise as therapeutic agents.[5−7]Alkylation of the pyridyl nitrogen of *meso*-(pyridyl)-porphyrins is one attractive synthetic strategy to generate cationic porphyrins.[8] Metalated *meso*-tetrakis(*N*-alkylpyridinium-2-yl)-porphyrins are of particular interest because they have been shown to have superior superoxide dismutase[9] and peroxynitrite decomposition properties[6] relative to those of the 3-pyridyl and 4-pyridyl isomers and high potency in animal models of inflammatory disease. The 2-pyridyl isomers also offer potential synthetic access to chiral metalloporphyrin scaffolds for use as water-soluble oxidation catalysts and hosts for chiral recognition.

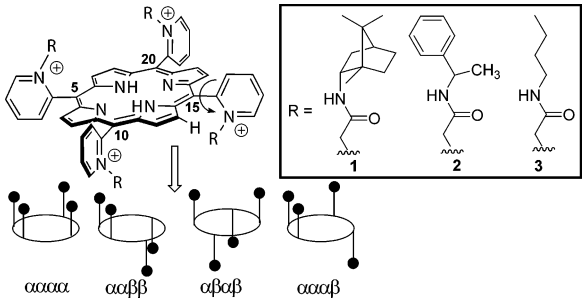

FIGURE 1. Hindered rotation in *meso*-tetrakis(*N*-alkylpyridinium-2-yl)-porphyrin leads to the existence of atropisomers. Inset: Alkyl substituents used in this study are shown.

The products of the alkylation of 2-pyridyl porphyrins are expected to be a mixture of four possible rotational isomers as a result of hindered interannular rotation of the pyridyl groups with respect to the porphyrin plane (Figure 1).[10,11] The statistical distribution of the αααα, ααα*β*, αα*ββ*, and α*β*α*β* atropisomers is 12.5%, 50%, 25%, and 12.5%, respectively, and mixtures with similar distributions are generally observed in porphyrin synthesis.[12,13] For enantioselective catalysis[10,14] and chiral recognition in water,[3] the αα*ββ* or the α*β*α*β* atropisomers are highly desirable because of their intrinsic symmetry. Given the potential applications of these compounds, it would be particularly useful to develop strategies for the facile assembly of a single rotational isomer of *N*-functionalized *meso*-tetrakis-2-pyridinium porphyrins.

Isolable atropisomers are generally obtained with *ortho*-substituted *meso*-phenyl porphyrins.[10,15] In practice, atropisomer ratios have been shown to deviate from the statistical distributions in some cases,[16−18] and strategies employing thermodynamic effects have afforded practical approaches to both α*β*α*β* and αα*ββ* atropisomers.[19−23] However, the atropisomers of water-

(1) Meunier, B.; de Visser, S. P.; Shaik, S. *Chem. Rev.* **2004**, *104*, 3947−3980.
(2) Jin, N.; Groves, J. T. *J. Am. Chem. Soc.* **1999**, *121*, 2923−2924.
(3) Imai, H.; Munakata, H.; Uemori, Y.; Sakura, N. *Inorg. Chem.* **2004**, *43*, 1211−1213.
(4) Mizutani, T.; Wada, K.; Kitagawa, S. *J. Am. Chem. Soc.* **1999**, *121*, 11425−11431.
(5) Batainić-Haberle, I.; Spasojević, I.; Stevens, R. D.; Hambright, P.; Neta, P.; Okada-Matsumoto, A.; Fridovich, I. *Dalton Trans.* **2004**, 1696−1702.
(6) Szabó, C.; Mabley, J. G.; Moeller, S. M.; Shimanovich, R.; Pacher, P.; Virág, L.; Soriano, F. G.; Van Duzer, J. H.; Williams, W.; Salzman, A. L.; Groves, J. T. *Mol. Med.* **2002**, *8*, 571−580.
(7) Pandey, R. K.; Zheng, G. In *The Porphyrin Handbook*; Kadish, K., Smith, K., Guilard, R., Eds.; Academic Press: New York, 2000; Vol. 6, pp 157−230.
(8) Hambright, P.; Fleischer, E. B. *Inorg. Chem.* **1970**, *9*, 1757−1761.
(9) Batinić-Haberle, I.; Benov, L.; Spasojević, I.; Fridovich, I. *J. Biol. Chem.* **1998**, *273*, 24521−24528.
(10) Rose, E.; Andrioletti, B.; Zrig, S.; Quelquejeu-Ehtève, M. *Chem. Soc. Rev.* **2005**, *34*, 573−583.
(11) Spasojević, I.; Menzeleev, R.; White, P. S.; Fridovich, I. *Inorg. Chem.* **2002**, *41*, 5874−5881.
(12) Walker, F. A.; Avery, G. L. *Tetrahedron Lett.* **1971**, *12*, 4949−4952.
(13) Gottwald, L. K.; Ullman, E. F. *Tetrahedron Lett.* **1969**, *10*, 3071−3074.
(14) Meunier, B. *Chem. Rev.* **1992**, *92*, 1411−1456.
(15) Collman, J. P.; Brauman, J. I.; Doxsee, K. M.; Halbert, T. R.; Bunnenberg, E.; Linder, R. E.; LaMar, G. N.; Del Gaudio, J.; Lang, G.; Spartalian, K. *J. Am. Chem. Soc.* **1980**, *102*, 4182−4192.
(16) Crossley, M. J.; Field, L. D.; Forster, A. J.; Harding, M. M.; Sternhell, S. *J. Am. Chem. Soc.* **1987**, *109*, 341−348.
(17) Freitag, R. A.; Whitten, D. G. *J. Phys. Chem.* **1983**, *87*, 3918−3925.
(18) Hatano, K.; Anzai, K.; Kubo, T.; Tamai, S. *Bull. Chem. Soc. Jpn.* **1981**, *54*, 3518−3521.

10.1021/jo062017r CCC: $37.00
Published on Web 01/31/2007

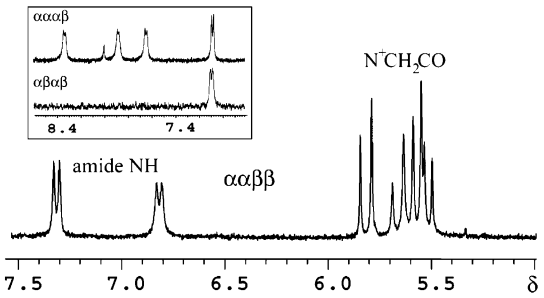

FIGURE 2. ^{1}H NMR of αα*ββ*-**1** showing the amide CON*H* and N^+CH_2CO protons. Inset: ^{1}H NMR spectra of the other atropisomers of **1** showing the amide CON*H* protons.

soluble cationic porphyrins have not been studied as extensively. Isomers of *meso*-tetrakis(*N*-methylpyridinium-2-yl)-porphyrin (2-TMPyP) have been characterized,[11,24−26] and statistical distributions of the atropisomers have also been observed.[11]

Here we report the preferential formation of a single atropisomer (the αα*ββ* isomer) as the major product in the synthesis of a series of novel cationic porphyrins (Figure 1, inset), obtained by alkylating 2-PyP with bromoacetamides. Two of these porphyrins have chiral alkyl groups (porphyrins **1** and **2**) and hence could be used as water-soluble chiral hosts or catalysts. The HPLC separation and characterization of the atropisomers of *N*-bornyl derivative **1** and its partially alkylated precursors were explored. The time course and *kinetic* preferences observed for the successive *N*-alkylations provide an explanation for the observed selectivity in the *N*-alkylation of 2-PyP.

2-Tetrakis(*N*-(*R*)-(+)-bornylacetamido)-pyridylporphyrin (2-TRBorPyP, **1**) was prepared by alkylating 2-PyP with (*R*)-bornylbromoacetamide (see Experimental Section). The reaction mixture was analyzed by ESI-MS, analytical reversed phase HPLC, and ^{1}H NMR. HPLC separation and ESI-MS of the separated products indicated the presence of three tetraalkylated (designated F_1, F_2, and F_4; see Figure 4) and one trialkylated porphyrin (T_1, 6.7% of reaction mixture). Analytical HPLC indicated that after 27 h at 100 °C, the relative abundances of the three tetraalkylated components were 79% (F_1), 16.4% (F_2), and 4.3% (F_4).

In the ^{1}H NMR spectrum of F_1 (Figure 2) the four amide CON*H* protons appear at *δ*6.7 (integration 2H) and *δ*7.3 (integration 2H) as doublets split by the adjacent proton on the bornyl group. The signals for enantiotopic N^+CH_2CO protons of the alkyl groups are also seen as a pair of overlapping AB quartets. In the case of the C_2-symmetric αα*ββ* isomer, the two chiral *ortho*-substituents on one face of the *meso*-tetrakis(2-pyridyl)-porphyrin are nonequivalent. These features of the spectrum prove definitively that the major tetraalkylated component (F_1) isolated by semipreparative HPLC is the αα*ββ* atropisomer.

Further proof for this assignment came from examination of the ^{1}H NMR spectra of the two other tetra-alkylated atropisomers (F_2 and F_4). The ^{1}H NMR for F_2 indicated no symmetry and clearly had four doublets for the four CON*H* protons (Figure 2, inset). The only compound that has no symmetry is the ααα*β* isomer. The spectrum for F_4 (Figure 2, inset), on the other hand, shows only one peak for each kind of proton. It had one doublet for the CON*H* protons that integrated to four and indicated that all of the amide protons were equivalent. This clearly indicated that the compound isolated (F_4) had D_2 or C_4 symmetry and hence could be either the αααα or the α*β*α*β* isomer.

Thus, we have unambiguously identified the αα*ββ* (F_1) and the ααα*β* (F_2) isomers. The order of HPLC elution for the four atropisomers of 2-TMPyP has been reported to be α*β*α*β*, αα*ββ*, ααα*β*, and then αααα.[11] For 2-TRBorPyP, the elution order on reversed phase HPLC was F_4, F_1 (αα*ββ*), and then F_2 (ααα*β*). F_4 was the first compound that eluted on the HPLC, and hence it is likely to be the α*β*α*β* compound. Also, since the alkylating groups for this compound are very bulky, the missing isomer is presumed to be αααα because of the extreme steric congestion expected for this arrangement of substituents. Thus, we assigned F_4 as α*β*α*β* (4%), F_1 as αα*ββ* (79%), and F_2 as ααα*β* (16.4%).

2-Tetrakis(*N*-(*R*)-(+)-methylbenzylacetamido)-pyridylporphyrin (2-TRMBzPyP, **2**) was prepared by alkylating 2-PyP with (*R*)-(+)-methylbenzylbromoacetamide. The simplicity of the ^{1}H NMR spectrum of both the crude reaction mixture and the purified porphyrin indicated that the mixture of atropisomers was biased toward one or two isomers rather than forming as a statistical mixture. The two differing methylbenzyl fragments show two sets of equally intense signals throughout all the regions of the ^{1}H NMR spectrum as expected for the αα*ββ* isomer (Figures S4−S7, Supporting Information). The relative abundance of αα*ββ*-**2** from HPLC was 44%.

2-TnBuPyP (**3**) was prepared by alkylating 2-PyP with *n*-butylbromoacetamide. Particularly diagnostic in the ^{1}H NMR spectrum was the appearance of the N^+CH_2CO protons as a set of two doublets near δ 5.5 (J_{AB} = 17 Hz) closely resembling an AB quartet (Figure S8, Supporting Information). Only the αα*ββ* isomer would be expected to give this splitting pattern since this arrangement has a C_2 axis of symmetry and a plane of symmetry (the alkylating groups are achiral). Workup afforded αα*ββ*-**3** in 69% isolated yield.

Atropisomerization of 2-TRMBzPyP (2) upon Prolonged Heating. The reaction for the synthesis of **2** was monitored over time by quenching the reaction at different time points and identifying the products by LC-ESI. The αα*ββ* isomer of 2-TRMBzPyP was identified by comparison to a stock sample of atropisomerically pure 2-TRMBzPyP obtained by semipreparative HPLC (top trace, Figure 3). At t = 4 h, at least nine partially alkylated and tetraalkylated products were evident. At t = 12 h, two major peaks appeared at 13.1 min (44% relative abundance from HPLC) and at 13.5 min (30% relative abundance from HPLC). Further heating caused the peak at 13.1 min to lose intensity relative to the peak at 13.5 min, indicating that isomerization was taking place (Figure 3).

The identity of the peak at 13.1 min was confirmed by its identical retention time, ^{1}H NMR spectrum, and ESI-MS as compared to a standard sample of αα*ββ* 2-TRMBzPyP. The peak at 13.5 min (also tetraalkylated from ESI-MS) was assigned

(19) Rose, E.; Ren, Q. Z.; Andrioletti, B. *Chem. Eur. J.* **2004**, *10*, 224−230.
(20) Zimmer, B.; Bulach, V.; Drexler, C.; Erhardt, S.; Hosseini, M. W.; De Cian, A. *New J. Chem.* **2002**, *26*, 43−57.
(21) Collman, J. P.; Wang, Z.; Straumanis, A.; Quelquejeu, M.; Rose, E. *J. Am. Chem. Soc.* **1999**, *121*, 460−461.
(22) Rose, E.; Cardon-Pilotaz, A.; Quelquejeu, M.; Bernard, N.; Kossanyi, A.; Desmazieres, B. *J. Org. Chem.* **1995**, *60*, 3919−3920.
(23) Lindsey, J. *J. Org. Chem.* **1980**, *45*, 5215−5215.
(24) Kachadourian, R.; Menzeleev, R.; Agha, B.; Bocckino, S. B.; Day, B. J. *J. Chromatogr. B* **2002**, *767*, 61−67.
(25) Dixon, D. W.; Pu, G.; Wojtowicz, H. *J. Chromatogr. A* **1998**, *802*, 367−380.
(26) Kaufmann, T.; Shamsai, B.; Lu, R. S.; Bau, R.; Miskelly, G. M. *Inorg. Chem.* **1995**, *34*, 5073−5079.

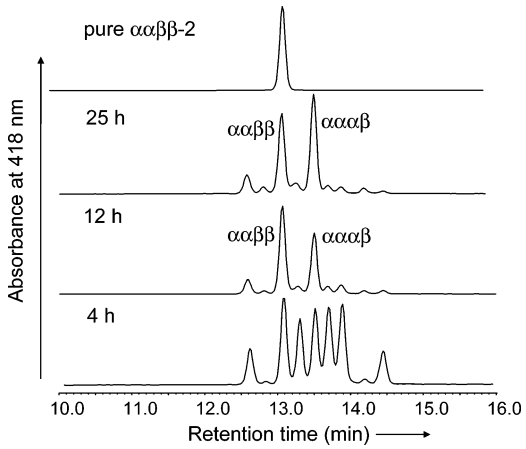

FIGURE 3. Reaction progress during the preparation of 2-TRMBzPyP (**2**) monitored by taking aliquots from the reaction mixture and analyzing by reversed phase HPLC.

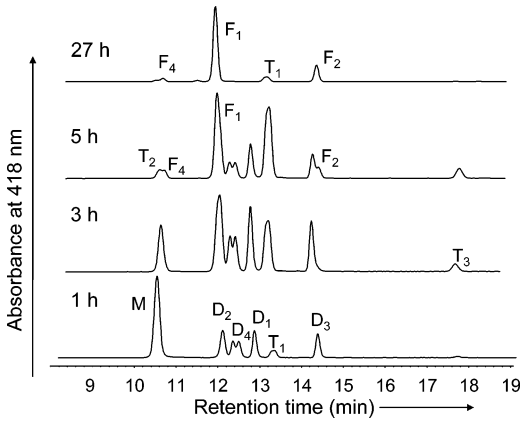

FIGURE 4. Formation of intermediates in the synthesis of 2-TRBorPyP (**1**) monitored by analytical HPLC. M = monoalkylated; D_1, D_2, D_3, D_4 = dialkylated; T_1, T_2, T_3 = trialkylated; F_1, F_2, F_4 = tetraalkylated.

to the αααβ isomer on the basis of its ^{1}H NMR, which showed that the molecule had no symmetry. This interpretation is further supported by the similar isomer elution pattern for 2-TRBorPyP (**1**). The loss of intensity at 13.1 min and the subsequent rise in the peak at 13.5 min over time indicates that the ααββ isomer will isomerize to αααβ with heating. The results presented here for 2-TRMBzPyP (**2**) support a kinetic effect during the alkylation reaction, since we observed that the ααββ isomer is enriched at an early point in the reaction and then isomerizes upon prolonged heating.

Probing the Mechanism Leading to the Unusual ααββ Alkylation Selectivity. Previously, an excess of a single isomer in the synthesis of uncharged, picket-fence porphyrins has been observed in a couple of cases. The mechanism of selectivity was attributed to either sterics or the separation technique.[13,16−18,23,27,28] In our studies, we have shown selectivity toward the ααββ isomer for three positively charged picket fence porphyrins with acetamide groups in the pickets. Since this is an intriguing and potentially useful result, we decided to probe the mechanism of this selectivity.

The progress of the reaction for the synthesis of 2-TRBorPyP (**1**) was monitored by looking at the various partially alkylated species formed during the reaction. This porphyrin was chosen for probing because we were able to identify the partially alkylated products formed during the course of the reaction. The reaction was monitored by taking aliquots of the reaction mixture at different time points, quenching them, and analyzing them by reversed phase HPLC. The extent of alkylation of the products formed was obtained by LC-ESI. The results are summarized in Figure 4, and the details of the identification of the intermediates have been included in Supporting information.

Figure 4 shows the time evolution of the various intermediates and products. From the HPLC integration values (assuming that these porphyrins have similar extinction coefficients), we can get relative abundances of the products and intermediates. We tried to look at the time point at which there was maximum dialkylation and obtain relative abundances of the dialkylated isomers. The same was done for the trialkylated intermediates. Table 1 compares the ratio of products obtained from this analysis with the expected statistical ratio. At the dialkylation stage, the four expected dialkylated products are formed in approximately equal amounts within the first 30 min of the reaction. Statistically, the ratio of 5,15-αα, 5,15-αβ, 5,10-αα, and 5,10-αβ (porphyrin *meso* positions are numbered as 5, 10, 15 and 20, Figure 1) should be 1:1:2:2. The fact that the dialkylated products are obtained in equal amounts indicates that there is a small preference for the formation of the 5,15 isomers over the 5,10 isomers in the dialkylation stage, which could be due to the fact that the positive charges are more separated in the 5,15 isomers. The three trialkylated products ααβ, αβα, and ααα should be formed in 50%, 25%, and 25% relative yields statistically. Table 1 shows that the deviation in the ratio of dialkylated products should not lead to any deviation from the statistical distribution for the ratio of trialkylated products obtained. The experimental abundances for the trialkylated products obtained after 5 h of reaction time are 83% ααβ, 6% αβα, and 11% ααα. Although some tetraalkylated product might already have formed at this time, the distribution indicates that the formation of the ααβ isomer is favored over the other two isomers and that there is a deviation from the statistical distribution that leads to an excess of the ααβ isomer. The final products of the reaction after 27 h of heating are αβαβ, ααββ, and αααβ in the relative abundances 4%, 79%, and 16% (by neglecting the presence of the trialkylated product left in the end of the reaction). These results indicate that the observed selectivity appeared in the tri- and tetraalkylation stages.

TABLE 1. Comparison of Experimental and Statistical Ratios of Intermediates and Products for the Synthesis of 2-TRBorPyP (1)

Di	Stat[a]	Expt[b]	Tri	Stat[c]	Expt[b]	Tetra	Stat[a]	Expt[b]
	16.6	25		50	83		25	79.3
	16.6	25		25	6		50	16.4
	33.3	25		25	11		12.5	-[d]
	33.3	25					12.5	4.3

[a] Statistical distribution. [b] Experimental distribution. [c] Expected ratio of trialkylated products from the experimental ratio of dialkylated products. [d] Not obtained in analytical HPLC separations.

(27) Freitag, R. A.; Mercer-Smith, J. A.; Whitten, D. G. *J. Am. Chem. Soc.* **1981**, *103*, 1226−1228.
(28) Elliott, C. M. *Anal. Chem.* **1980**, *52*, 666−668.

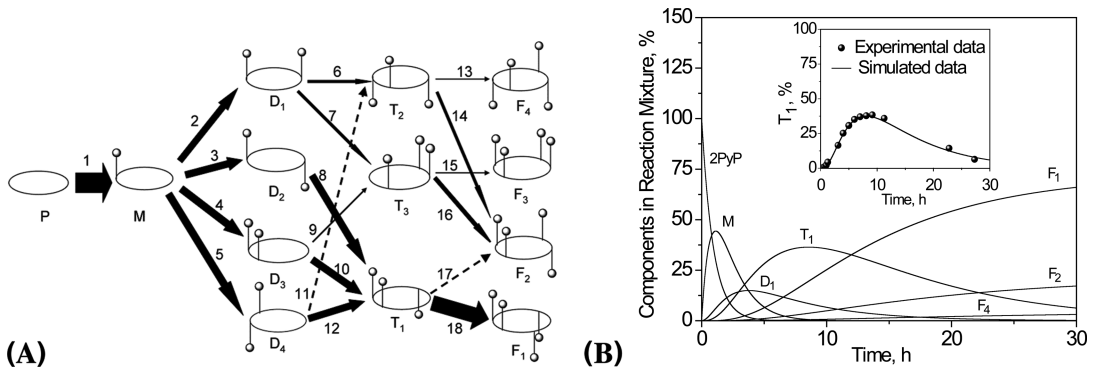

FIGURE 5. (A) Flowchart of reactions leading to the preferential formation of F_1, depicting the relative fluxes at each step based on estimates of the pseudo-first-order *N*-alkylation rate constants obtained from the simulations. The order of the rate constants are $k_1 = 10^{-4}$ s^{-1}; k_9, k_{13}, $k_{15} = 10^{-6}$ s^{-1}; k_{11}, $k_{17} = 10^{-8}$ s^{-1}; the rest of the rate constants were of the order 10^{-5} s^{-1}. (B) Kinetic simulations of the reactions leading to the experimental ratio of products obtained. Comparison of the experimental data for T_1 with the simulated data is shown in the inset.

The formation and disappearance of the several intermediate products of the alkylation reaction can be modeled to obtain relative rates. Modeling can provide further information on the mechanism underlying the selectivity. Before considering diastereomers and enantiomers, at least 12 products can be envisioned in this complex system. The scheme of reactions leading to the four tetraalkylated products is shown in Figure 5A as a flow diagram.

We used kinetic simulations to write chemical reactions, plot reaction profiles, and obtain values for the rate constants (see Supporting Information for details). Since we were able to identify most of the reaction intermediates leading to 2-TRBorPyP (**1**), the progress of the alkylation process could be determined from the HPLC data. The comparison of one of the simulated curves (Figure 5B, inset) shows that the results obtained from the simulations matched well with the experimental data (Figure 5B). These simulations indicate that the reaction rates for the conversion of intermediate D_4 to T_2 and that of T_1 to F_2 are at least 100 times slower than the other rates and hence should be the most significant cause of the unusual selectivity. In both of these steps the alkylating group has to approach on the same side as another alkylated pyridyl moiety, leading to a 5,15-αα interaction. Thus, the experimental results and simulations indicate that 5,15-αα alkylation is disfavored in the tri- and tetraalkylation stages and is the cause for the observed selectivity in these stages.

An explanation for the slow rate of 5,15-αα alkylation can be inferred if we consider the ruffling of the porphyrin ring. Ruffling is the structural deformation observed in *meso*-substituted porphyrins in which the macrocycle is markedly nonplanar with the *meso* carbons moving alternately up and down out of the porphyrin plane.[29−32] The magnitude of the porphyrin ruffling depends on the bulkiness of the *meso* substituents. As the number of alkyl groups increases during the formation of the tetraalkylated product, the steric bulk of the *meso* positions of the porphyrin ring also increases, and hence, the extent of deformation should increase with successive alkylation. When the trialkylated porphyrin is formed from the dialkylated porphyrin, the magnitude of this deformation is high enough to sterically hinder further a 5,15-αα alkylation, since the 2-pyridyl nitrogens in the 5 and 15 positions are brought closer. The nitrogens on the 5 and 10 positions, on the other hand, become more separated as a result of this ruffling and hence 5,10-αα alkylation should be relatively less hindered.

In summary, we report the synthesis and characterization of three water-soluble *N*-acetamido-2-pyridinium porphyrins by alkylating 2-PyP. In each case we obtained the αα*ββ* isomer as the major product. The results support a kinetic effect during later stages of the sequential *N*-alkylation reaction. Finally, these results and the kinetic simulations indicate that the 5,15-αα alkylation is disfavored at the tri- and tetraalkylation stages and this is the reason for the observed selectivity. The results are significant since they open an avenue for using the *N*-alkylation of 2-PyP as a simple route to a single atropisomer that can then be used as a chiral host, asymmetric catalyst, or a drug candidate.

Experimental Section

Generic Route for Porphyrin Synthesis. Porphyrins **1**−**3** were synthesized by alkylating *meso*-tetrakis(2-pyridyl)-porphyrin (2-PyP) with either the *N*-(*R*)-bornyl, *N*-(*R*)-methylbenzyl, or *N*-*n*-butyl-α-bromoacetamides. The reaction mixtures were stirred in anhydrous DMF at 95−110 °C under argon until the porphyrin Soret band shifted to $\lambda = 418-420$ nm (solvent methanol). The reaction mixtures were analyzed by ESI-MS, analytical reversed phase HPLC, LC-ESI, and ^{1}H NMR. The separated atropisomers and partially alkylated products were identified by ESI-MS and ^{1}H NMR and from the analytical HPLC retention times. The details of the synthesis and characterization are provided in Supporting Information.

Acknowledgment. Support for this work by the National Institutes of Health (GM 36298) and the National Science Foundation (CHE-031630) is gratefully acknowledged. The authors thank Dr. Saw Kyin and Dr. Dorothy Little for help in obtaining ESI-MS and LC-ESI data. High-resolution mass spectrometry was provided by the Washington University Mass Spectrometry Resource with support from the NIH National Center for Research Resources (Grant P41RR0954).

Supporting Information Available: Synthesis, characterization, separation conditions, and kinetic modeling. This material is available free of charge via the Internet at http://pubs.acs.org.

JO062017R

(29) Sakai, T.; Ohgo, Y.; Hoshino, A.; Ikeue, T.; Saitoh, T.; Takahashi, M.; Nakamura, M. *Inorg. Chem.* **2004**, *43*, 5034−5043.
(30) Senge, M. O. *Z. Naturforsch., B: Chem. Sci.* **2000**, *55*, 336−344.
(31) Sánchez-Migallón, A.; de la Hoz, A.; Begtrup, M.; Fernández-Castaño, C.; Foces-Foces, C.; Elguero, J. *Tetrahedron* **1996**, *52*, 10811−10822.
(32) Werner, A.; Sánchez-Migallón, A.; Fruchier, A.; Elguero, J.; Fernández-Castaño, C.; Foces-Foces, C. *Tetrahedron* **1995**, *51*, 4779−4800.